1 mL, 50,000 copies/mL) were purchased from Zepto-Metrix (Buffalo, NY) and were diluted with defibrinated plasma to give a final concentration of 1 to 1000 copies/mL. Blood specimens from healthy volunteer donors who were confirmed as negative for HCV, HBV, and HIV were provided from Japan Red Cross and used as a negative control.

DNA and RNA extraction, reverse transcription, and PCR amplification

Each viral DNA and RNA was extracted from 200 μL of diluted sample with a viral nucleic acid kit and a viral RNA kit (High Pure, Roche, Basel, Switzerland). Total RNA of HCV, HIV-1, and WNV were all reverse transcribed with a cDNA synthesis kit (Superscript III RT, Invitrogen) according to the manufacturer's protocol. Twenty-microliter cDNA samples were prepared for PCR amplification of each virus. The PCR was carried out with PCR mixture (GoTaq, Promega, Madison, WI). In the PCR mixture, diluted nucleic acid and 50 μmol/L of each degenerate primer were included. The reaction consisted of 50 cycles of 94°C for 30 seconds, 55°C for 30 seconds, and 72°C for 60 seconds. We used 5 ng of human cDNA fragment as an internal control (IC).

Microchip fabrication

We purchased 3-mm^2 silicon DLC-chip from Toyo Kohan (Tokyo, Japan). Each probe was spotted by Spotarray 72 (Perkin-Elmer, Waltham, MA) with a 250-μm spot distance and 100-μm-diameter spots. Spotted probes were baked for 60 minutes at 80°C. We made DNA chips to evaluate probe sensitivity and for detection of viral samples, including WHO International Standards and WHO genotype panels. Each sequence for detection probes on the chip is listed in Table 2.

Synthesis and hybridization of fluorescently labeled DNA samples

PCR amplification of extracted DNA or cDNAs was performed for fluorescent labeling using polymerase (GoTaq, Promega) with Cy-5 dCTP. The PCR mixture included template DNA or cDNA, 50 μmol/L primers, 0.5 μL of Cy-5 dCTP (Perkin-Elmer), 1 μL of dNTP mixture (2.5 mmol/L each, 0.25 mmol/L dCTP), 5 μL of 5× PCR buffer (GoTaq, Promega), and 0.25 μL of polymerase (GoTaq, Promega). The 50-cycle PCR profile was 94°C for 30 seconds, 55°C for 30 seconds, and 72°C for 30 seconds. Amplification was carried out in a PCR system (GeneAmp 9700, Applied Biosystems, Foster City, CA). Two microliters of the PCR-amplified reaction mixture was hybridized with the chip for 30 minutes at 50°C. The hybridized chip was washed with saline-sodium citrate buffer and scanned with a fluorescent scanner (FLA-8000, Fujifilm, Tokyo, Japan). Geographic origin was estimated from the obtained fluorescence patterns, thereby indicating specific genotypes.

Transcription-mediated amplification assay

To validate our assay sample preparation including viral DNA or RNA, we performed transcription-mediated amplification (TMA) assays for HBV, HCV, and HIV-1 by using an assay kit (Ultrio, Novartis Pharma, Tokyo, Japan) according to the manufacturer's protocol.

RESULTS

Synthesis of genotype panel oligomers by OE-PCR

To verify our designed dPCR primers, we prepared genotype panel oligomers (100-300 bp) as viral genotype reference materials for HIV (A1, A2, B, C, D, F1, F2, G, H, J, K, N, O, and U), HBV (A–H), WNV (1-10), and PVB19 (1-6) made by OE-PCR (Fig. 1A). The target regions for OE-PCR were selected according to the nucleotide sequences of the standard strain for dPCR and the DLC-chip detection system (Supplemental Table S2). The joining oligonucleotides were designed using an online computer program (DNAWorks, Version 2, http://helixweb.nih.gov/dnaworks/). The nucleotide sequences of each genotype panel oligomer are listed in Supplemental Table S1. OE-PCR was carried out according to a two-step reaction method. The OE-PCR products were checked on a chip electrophoresis system (Multina 202, Shimazu). As expected, we could detect our OE-PCR products at appropriate molecular size (Fig. 1B). For HCV (1A, 2A, 3A, 4A, 6B, 6K, 6P, 6T, and 7A), genotype panel oligomers were designed and made by custom service (Invitrogen).

Validation of dPCR primer for detection of virus genotype panel oligomers

We confirmed whether our designed primers could specifically amplify each virus subtype by PCR. The PCR products for all HIV, HCV, HBV, PVB19, and WNV subtypes were detected at the expected size by gel electrophoresis (Fig. 1C).

QC of our pathogen detection DNA microarray system

To evaluate specificity of each probe in our DLC-chip, the detection ability of our probes was analyzed. We selected 36 specific probe sets that had high detection abilities (>50% of genotypes) from the 53 originally designed evaluated probes (data not shown) and then spotted them on DLP-Chip (Fig. 2A, B). DNA microarray images were

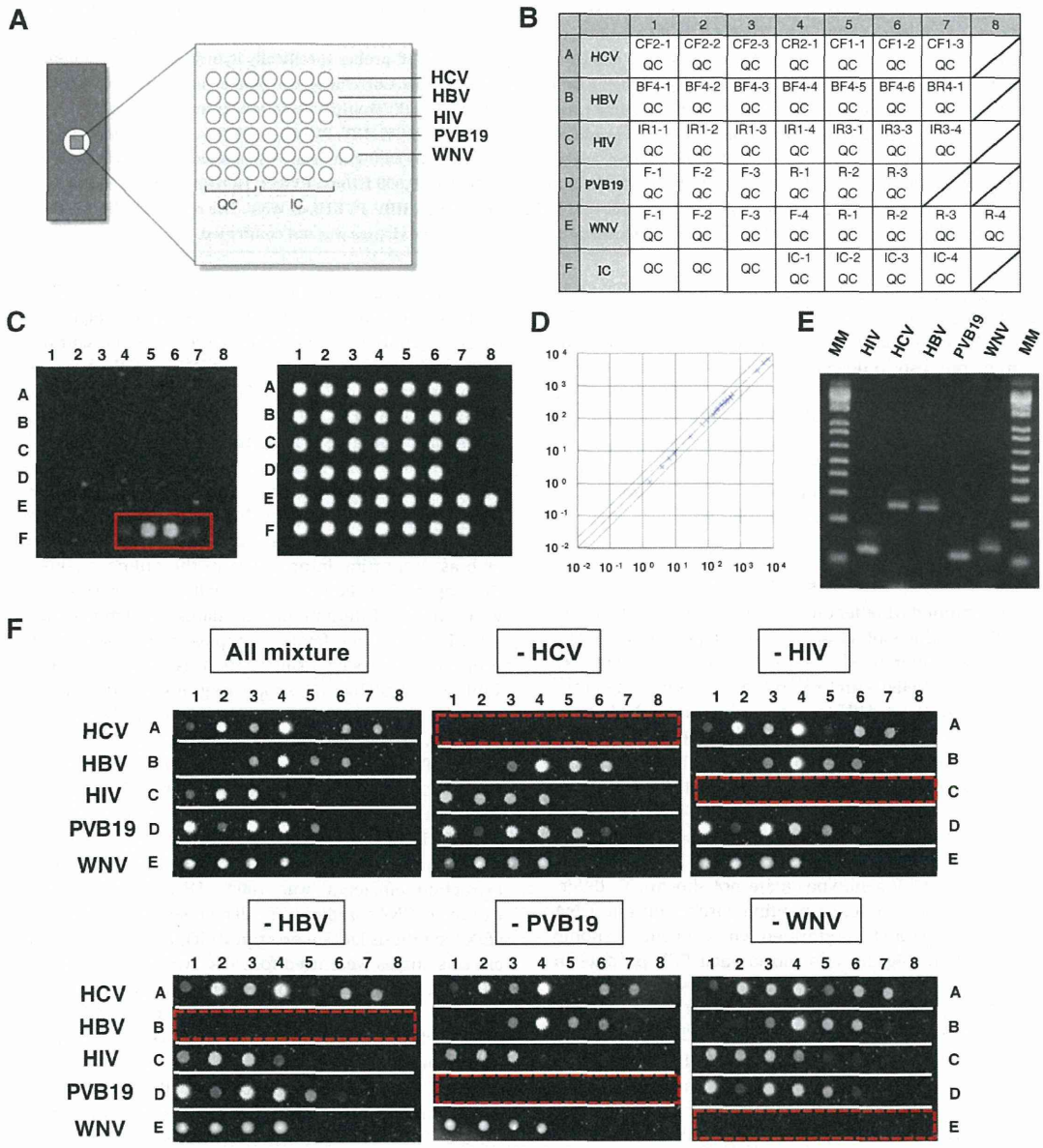

		1	2	3	4	5	6	7	8
A	HCV	CF2-1 QC	CF2-2 QC	CF2-3 QC	CR2-1 QC	CF1-1 QC	CF1-2 QC	CF1-3 QC	
B	HBV	BF4-1 QC	BF4-2 QC	BF4-3 QC	BF4-4 QC	BF4-5 QC	BF4-6 QC	BR4-1 QC	
C	HIV	IR1-1 QC	IR1-2 QC	IR1-3 QC	IR1-4 QC	IR3-1 QC	IR3-3 QC	IR3-4 QC	
D	PVB19	F-1 QC	F-2 QC	F-3 QC	R-1 QC	R-2 QC	R-3 QC		
E	WNV	F-1 QC	F-2 QC	F-3 QC	F-4 QC	R-1 QC	R-2 QC	R-3 QC	R-4 QC
F	IC	QC	QC	QC	IC-1 QC	IC-2 QC	IC-3 QC	IC-4 QC	

captured by an image analyzer (FLA-8000, Fuji Photo Film, Tokyo, Japan). Hybridized slides were inserted in the FLA-800, and the scan conditions were set as 10 μm resolution, standard scan mode, and photomultiplier tube high-value 100% laser. Saved DNA microarray images were analyzed, and fluorescent intensity of each spot was measured using a computer program (ArrayGauge Software, Fuji Photo Film). After removing the background signal, we defined the positive signal standard as radio intensity more than five times higher than background. The signal intensity was calculated as the total pixel value minus the global background. The signal intensities were then normalized to the mean for all the spots in the array.

To determine the specificity of the new system, we applied two different QCs: an IC probe (oligonucleotide complementary to the Cy5-labeled amplicon of the 18S

Fig. 2. (A) Schematic design of DLC-chip, including HIV, HCV, HBV, WNV, and PVB19 probes (B) and their relative position in the slide layout. Spotted probes of seven subtypes of HIV-1, seven genotypes of HCV, seven genotypes of HBV, six genotypes of PVB19, and eight genotypes of WNV were selected. All of the probes were spotted together on the chip, along with the QC probes. (C) Evaluation of the detection system using the IC (left panel) and QC (right panel). Anti-IC probes specifically hybridized to and amplified 18S rRNA PCR product from human DNA. (D) QC by using same amplified sample. Correlation coefficients using scatter plot indicated that each DLC-chip was highly reproducible, with a correlation of 0.99905. (E) Multiple detection system for five virus genomes. Agarose gel electrophoresis analysis of PCR products to detect HIV-1, HCV, HBV, PVB19, and WNV. These PCR products were positive on the microarrays. (F) Multiple detection system for five viruses by DLC-chip. The PCR products of five viruses were mixed at the following concentrations: HCV, 10 IU/mL; HBV, 10 IU/mL; HIV-1, 10,000 IU/mL; PVB19, 10 IU/mL; and WNV, 10 copies/mL. Each panel used a mixture of the five viruses that lacked HIV-1, HCV, HBV, PVB19, or WNV. The red line indicates the row where excluded virus was not detected. Cross-hybridization between the five viruses was not confirmed.

rRNA gene; Fig. 2C, left) and a QC probe (oligonucleotide complementary to the Cy3-labeled QC probe; Fig. 2C right). This allowed us not only to monitor the spot uniformity, but also to detect potential irregularities during the hybridization process. To evaluate the reproducibility of our DLC-chip, we hybridized the same PCR-amplified samples to different DLC-chips and measured each signal intensity. Correlation coefficients using scatter plots indicated that each DLC-chip was highly reproducible, showing a correlation of 0.99905 (Fig. 2D).

Multiple detection of five viruses in one test

We determined whether our designed probes could detect the PCR products of all the HIV genotypes. On the DLC-chip, seven different HIV-1–specific probes were aligned. After being labeled with Cy5, PCR products were detected by hybridization to HIV-specific probes on the DLC-chip. We considered that a sample was positive if at least two different probes showed a positive signal. These HIV-1–specific degenerative primer and probe sets detected all of the following genotypes: A1, A2, B, C, D, F1, F2, G, H, J, K, N, O, and U (data not shown). Similar to the HIV detection system, different probe sets detected all the HCV, HBV, PVB19, and WNV genotypes (data not shown). To determine the ability to detect multiple viruses on one DNA chip, we separately performed virus-specific genome amplification (Fig. 2E) and mixed each PCR product in one tube and hybridized the PCR products onto the DLC-chip. The mixed viral PCR product (HIV, HCV, HBV, PVB19, and WNV) was readily detected as a hybridized spot on the DCL-chip (Fig. 2F). We prepared a mixed sample minus one virus amplicon as a negative control for cross-hybridization and nonspecific binding. We confirmed that no cross-hybridization occurred with HIV-1, HCV, HBV, PVB19, and WNV.

Specificity and sensitivity of our dPCR-NAT system by using WHO genotype panels and international standards

To determine the specificity of our DNA microarray system to detect each virus genotype, we prepared the WHO genotype panel samples for each virus. For WNV, we used the genotype panel oligomer described in Figure 1 as an NAT genotype panel because there was no commercially available panel. We extracted DNA or RNA from each genotype panel for HIV, HCV, HBV, PVB19, and WNV. Each template DNA or cDNA was amplified with each dPCR primer listed in Table 1. The amplified PCR products for all genotypes of each virus were confirmed on 3% agarose gels and DNA chips. We detected all the HIV, HCV, HBV, PVB19, and WNV genotypes (Fig. 3B). Our DNA microarray data are summarized in Supplemental Table S4 (available as supporting information in the online version of this paper). To validate the sensitivity of our NAT system, we used WHO International Standards as reference materials. To check our reference samples, we performed FDA-licensed NAT assays using a TMA assay (Supplemental Table S3, available as supporting information in the online version of this paper) before analysis. For sensitivity assay, we prepared HCV RNA, HBV, and PVB19 from NIBSC. These materials were used as international standards for NAT quality assurance. We prepared each sample to give a final concentration of 1 to 10,000 IU/mL and isolated DNA or RNA from 200-μL samples. Thus, each sample was assumed to contain 0.2 to 2000 IU virus if extraction efficiency was 100%. DNA and RNA were extracted. RNA samples were all reverse transcribed with a cDNA synthesis kit (Superscript III RT, Invitrogen), and all cDNA samples were used for PCR. We detected 1 IU/mL HCV, 1 IU/mL HBV, 1 IU/mL PVB19, and 1 copy/mL WNV (Fig. 3C). Similar results were obtained from at least three independent experiments. For HIV, we estimated the detection limit in at least five independent tests. We detected 10,000 IU/mL for 100%, 1000 IU/mL for 77%, 100 IU/mL for 7%, 10 IU/mL for 0%, and 1 IU/mL sample for 0%. Thus we conclude that our system could detect 1000 IU/mL equivalent to 200 IU/PCR sample for HIV. Detection limits for each virus are listed in Table 3.

DISCUSSION

We investigated the performance of the new NAT system using dPCR primers and a DLC-chip. We showed that our NAT system was specific for HIV-1, HCV, HBV, PVB19, and

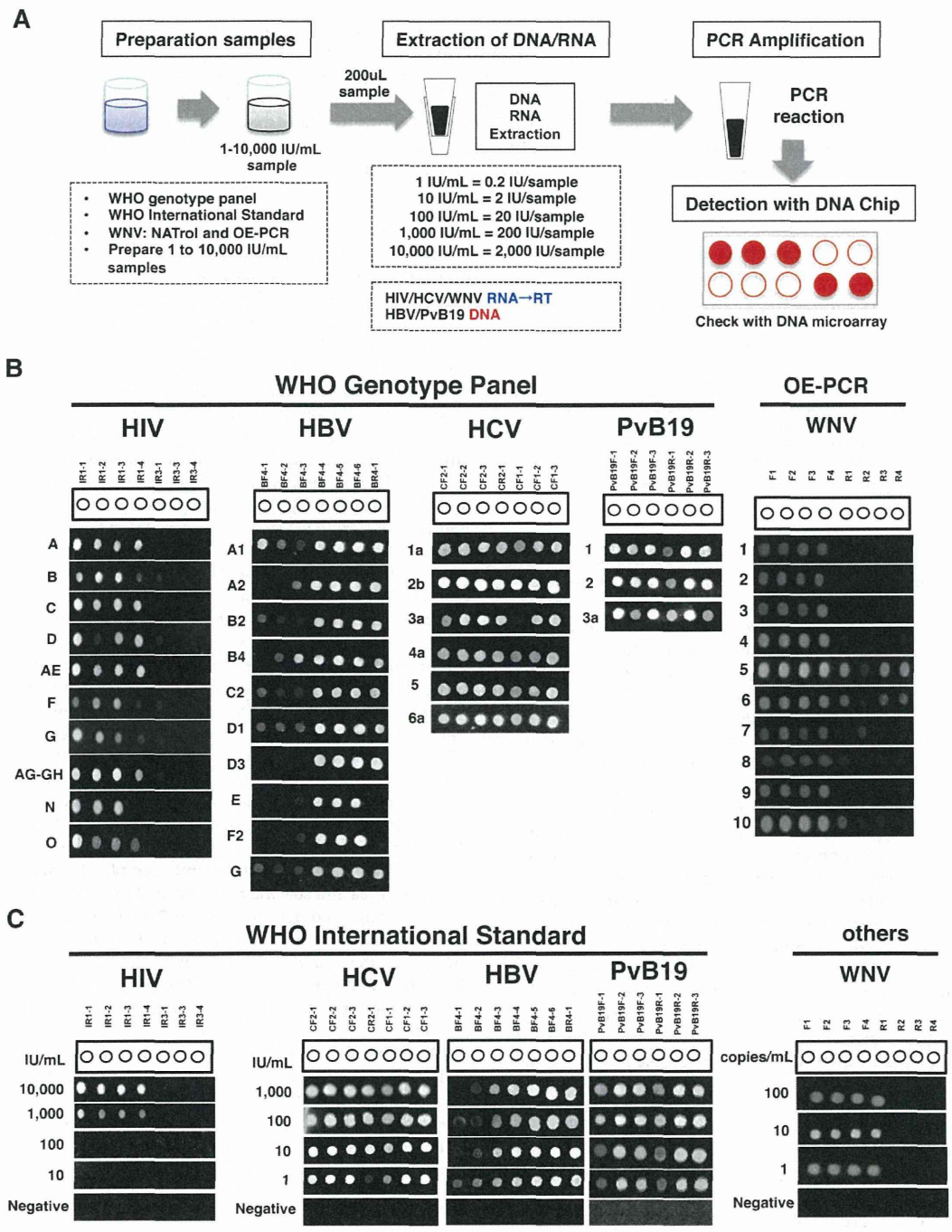
A
Preparation samples
Extraction of DNA/RNA
PCR Amplification
200uL sample
DNA RNA Extraction
PCR reaction
1-10,000 IU/mL sample
WHO genotype panel
WHO International Standard
WNV: NATrol and OE-PCR
Prepare 1 to 10,000 IU/mL samples
1 IU/mL = 0.2 IU/sample
10 IU/mL = 2 IU/sample
100 IU/mL = 20 IU/sample
1,000 IU/mL = 200 IU/sample
10,000 IU/mL = 2,000 IU/sample
HIV/HCV/WNV RNA→RT
HBV/PvB19 DNA
Detection with DNA Chip
Check with DNA microarray
B
WHO Genotype Panel
OE-PCR
HIV
HBV
HCV
PvB19
WNV
A
B
C
D
AE
F
G
AG-GH
N
O
A1
A2
B2
B4
C2
D1
D3
E
F2
G
1a
2b
3a
4a
5
6a
1
2
3a
1
2
3
4
5
6
7
8
9
10
C
WHO International Standard
others
HIV
HCV
HBV
PvB19
WNV
IU/mL
10,000
1,000
100
10
Negative
IU/mL
1,000
100
10
1
Negative
copies/mL
100
10
1
Negative

Fig. 3. (A) Schematic illustration of sensitivity analysis of our detection system, including extraction process. Detection of the isolated virus genomes from human plasma sample. Samples containing HIV-1, HCV, and HBV were diluted with defibrinated plasma (Basematrix 53; SeraCare) at 1 to 10,000 IU/mL. (B) For more accurate analysis, we prepared a WHO genotype panel for HIV-1, HBV, HCV, and PVB19. We detected all genotypes by using our designed degenerated primer. (C) For sensitivity analysis of our NAT system, we prepared WHO International Standards for HIV-1, HCV, HBV, and PVB19. We diluted these materials with negative sera at 1 to 10,000 IU/mL and extracted DNA and RNA from 200-μL samples. All RNA samples were transcribed with Superscript III. We detected HIV at 1000 IU/mL, HCV at 1 IU/mL, HBV at 1 IU/mL, and PVB19 at 1 IU/mL.

TABLE 3. Detection limit of our dPCR-NAT system*

IU/mL	HIV (%)	HCV (%)	HBV (%)	PVB19 (%)
10,000	100	100	100	100
1,000	77	100	100	100
100	7	100	100	100
10	0	100	100	100
1	0	50	25	75

* % positive: Reactive/Tested (Percent Reactive). The measurement obtained in each specimen was tested with two sample lots in two independent test assays. For HIV, we tested five sample lots in five independent test assays.

WNV at low viral loads. In addition, we showed that our system detected various virus genotypes. Degenerate primers are useful not only for detecting unknown genes, but also for the simultaneous amplification of mutated genes.[17] In the case of viruses, many mutated strains appear in a particular geographical area and at a specific time.[18] Recently, we used CoCoMo primers, a fully automatic design pipeline for PCR primers, according to the CodeHop primer design strategy, by which others can analyze the oligonucleotide motif incidence.[14] The CoCoMo program is available online (www.geneknot.info/cocomo). We utilized CoCoMo primers to design the primer sequences in this study. The algorithm-designed primers were confirmed to fit most subtypes or genotypes of the target viruses (Table 1) and enabled efficient detection of a wide range of viruses. In general, PCR procedures with the degenerate primers had lower sensitivity than that of the specific primers. To overcome this disadvantage, we used fluorescence detection on the DLC-chip, which provided higher sensitivity.[12] Additionally, the degenerate primer set was designed to detect the polymorphic region of the viral genome; therefore, subtypes or genotypes could be discriminated on the DLC-chip. The combination of the primers and DLC-chips was therefore validated. These results suggest that the combination of dPCR and DLC-chips is beneficial for blood-borne virus detection. To increase the safe use of the system, automation of our detection system will be required in the future.

A low level of HBV may proliferate in transfused recipients who are immunocompromised or immunosuppressed. In addition, the window period of HBV is relatively long, but the presence of HBV DNA without detectable HBsAg outside the window period, known as occult HBV infection, has been reported.[7] This suggests that the development of a highly sensitive detection system for HBV is particularly important. Although the current TMA sensitivity corresponds to 1 to 5 IU/mL at the reproductive level, using the same viral samples in this study we detected 1 to 10 IU/mL HBV. These data suggest that the sensitivity of our analysis system is equivalent to that of the TMA assay (Fig. 3C). Thus far, HBV Genotype C is the most prevalent genotype in Japan (85%), while the prevalence of Genotypes A and D is 1.7 and 0.4%, respectively.[19-21] Currently, the level of Genotype A is increasing in the younger generation because of horizontal infection.[11,22,23]

For HIV-1 detection and quantification, various methods have been developed, but most real-time techniques involve their sensitivity to point mutations within primer and probe target sequences. Our dPCR-NAT system could detect a wide range of HIV genotypes by using dPCR primers. Despite the wide range of genotype detection, sensitivity was not high. We could detect 200 IU HIV/PCR procedure. Improvement is needed for HIV dPCR sensitivity. Similarly for HBV and HCV, the next-generation virus detection system must be able to cope with this situation, namely, by possessing a wide detectable viral genotype range and a low detection level. With our detection system, all of the virus genotypes were detected at 1 to 1000 IU/mL sample. Previous studies by Hsia and coworkers[24] combined multiplex PCR and DNA chips and detected three different viruses in a single sample. Our mixed PCR product data (Fig. 2F) indicated that our system could simultaneously detect five different viruses in one DNA chip. These data suggest that our system is suitable for multiple pathogen testing.

In conclusion, the dPCR-NAT system is an accurate and reliable test for HIV, HBV, HCV, PVB19, and WNV detection with respect to specificity, sensitivity, and genotype inclusivity and a reproducible assay for the detection of multiple blood-contaminating pathogens.

ACKNOWLEDGMENT

We are grateful for the advice and support of Dr Makoto Handa (Keio University).

CONFLICT OF INTEREST

All authors concur with submission of this manuscript, and we affirm that the material submitted has not previously been reported, and is not under consideration for publication elsewhere. We do not have any conflicting financial interests.

REFERENCES

1. Tabor E, Epstein JS. NAT screening of blood and plasma donations: evolution of technology and regulatory policy. Transfusion 2002;42:1230-7.
2. Stramer SL, Hollinger FB, Katz LM, Kleinman S, Metzel PS, Gregory KR, Dodd RY. Emerging infectious disease agents and their potential threat to transfusion safety. Transfusion 2009;49(Suppl 2):1S-29S.
3. Lelie PN, Cuypers HTM, van Drimmelen AAJ, Quint WGV. Quality assessment of hepatitis C virus nucleic acid amplification methods. Infus Ther Transfus Med 1998;25:102-10.
4. Fischer SA. Emerging viruses in transplantation: there is more to infection after transplant than CMV and EBV. Transplantation 2008;86:1327-39.
5. Kramvis A, Kew M, François G. Hepatitis B virus genotypes. Vaccine 2005;23:2409-23.
6. Norder H, Couroucé AM, Coursaget P, Echevarria JM, Lee SD, Mushahwar IK, Robertson BH, Locarnini S, Magnius LO. Genetic diversity of hepatitis B virus strains derived worldwide: genotypes, subgenotypes, and HBsAg subtypes. Intervirology 2004;47:289-309.
7. Allain JP. Occult hepatitis B virus infection: implications in transfusion. Vox Sang 2004;86:83-91.
8. Pealer LN, Marfin AA, Petersen LR, Lanciotti RS, Page PL, Stramer SL, Stobierski MG, Signs K, Newman B, Kapoor H, Goodman JL, Chamberland ME. West Nile Virus Transmission Investigation Team. Transmission of West Nile virus through blood transfusion in the United States in 2002. N Engl J Med 2003;349:1236-45.
9. Grinev A, Daniel S, Stramer S, Rossmann S, Caglioti S, Rios M. Genetic variability of West Nile virus in US blood donors, 2002-2005. Emerg Infect Dis 2008;14:436-44.
10. Candotti D, Temple J, Owusu-Ofori S, Allain JP. Multiplex real-time quantitative RT-PCR assay for hepatitis B virus, hepatitis C virus, and human immunodeficiency virus type 1. J Virol Methods 2004;118:39-47.
11. Kobayashi M, Ikeda K, Arase Y, Suzuki F, Akuta N, Hosaka T, Sezaki H, Yatsuji H, Kobayashi M, Suzuki Y, Watahiki S, Mineta R, Iwasaki S, Miyakawa Y, Kumada H. Change of hepatitis B virus genotypes in acute and chronic infections in Japan. J Med Virol 2008;80:1880-4.
12. Gao Y, Chen X, Gupta S, Gillis KD, Gangopadhyay S. Magnetron sputtered diamond-like carbon microelectrodes for on-chip measurement of quantal catecholamine release from cells. Biomed Microdevices 2008;10:623-9.
13. Iwafune Y, Tan JZ, Ino Y, Okayama A, Ishigaki Y, Saito K, Suzuki N, Arima M, Oba M, Kamei S, Tanga M, Okada T, Hirano H. On-chip identification and interaction analysis of gel-resolved proteins using a diamond-like carbon-coated plate. J Proteome Res 2007;6:2315-22.
14. Jimba M, Takeshima SN, Matoba K, Endoh D, Aida Y. BLV-CoCoMo-qPCR: quantitation of bovine leukemia virus proviral load using the CoCoMo algorithm. Retrovirology 2010;7:91.
15. Hoover DM, Lubkowski J. DNAWorks: an automated method for designing oligonucleotides for PCR-based gene synthesis. Nucleic Acids Res 2002;30:e43.
16. Dong B, Mao R, Li B, Liu Q, Xu P, Li G. An improved method of gene synthesis based on DNA works software and overlap extension PCR. Mol. Biotechnol 2007;37:195-200.
17. Moonka D, Loh EY. A consensus primer to amplify both alpha and beta chains of the human T cell receptor. J Immunol Methods 1994;169:41-51.
18. Ha C, Coombs S, Revill PA, Harding RM, Vu M, Dale JL. Design and application of two novel degenerate primer pairs for the detection and complete genomic characterization of potyviruses. Arch Virol 2008;153:25-36.
19. Orito E, Ichida T, Sakugawa H, Sata M, Horiike N, Hino K, Okita K, Okanoue T, Iino S, Tanaka E, Suzuki K, Watanabe H, Hige S, Mizokami M. Geographic distribution of hepatitis B virus (HBV) genotype in patients with chronic HBV infection in Japan. Hepatology 2001;34:590-4.
20. Sugauchi F, Kumada H, Sakugawa H, Komatsu M, Niitsuma H, Watanabe H, Akahane Y, Tokita H, Kato T, Tanaka Y, Orito E, Ueda R, Miyakawa Y, Mizokami M. Two subtypes of genotype B (Ba and Bj) of hepatitis B virus in Japan. Clin Infect Dis 2004;38:1222-8.
21. Sugauchi F, Kumada H, Acharya SA, Shrestha SM, Gamutan MT, Khan M, Gish RG, Tanaka Y, Kato T, Orito E, Ueda R, Miyakawa Y, Mizokami M. Epidemiological and sequence differences between two subtypes (Ae and Aa) of hepatitis B virus genotype A. J Gen Virol 2004;85:811-20.
22. Yoshikawa A, Gotanda Y, Suzuki Y, Tanaka M, Matsukura H, Shiraishi T, Matsubayashi K, Kon E, Suzuki K, Yugi H; Japanese Red Cross HBV Genotype Research Group. Age- and gender-specific distributions of hepatitis B virus (HBV) genotypes in Japanese HBV-positive blood donors. Transfusion 2009;49:1314-20.
23. Matsuura K, Tanaka Y, Hige S, Yamada G, Murawaki Y, Komatsu M, Kuramitsu T, Kawata S, Tanaka E, Izumi N, Okuse C, Kakumu S, Okanoue T, Hino K, Hiasa Y, Sata M, Maeshiro T, Sugauchi F, Nojiri S, Joh T, Miyakawa Y, Mizokami M. Distribution of hepatitis B virus genotypes among patients with chronic infection in Japan shifting toward an increase of genotype A. J Clin Microbiol 2009;47:1476-83.
24. Hsia CC, Chizhikov VE, Yang AX, Selvapandiyan A, Hewlett I, Duncan R, Puri RK, Nakhasi HL, Kaplan GG. Microarray multiplex assay for the simultaneous detection and discrimination of hepatitis B, hepatitis C, and human immunodeficiency type-1 viruses in human blood samples. Biochem Biophys Res Commun 2007;356:1017-23.

SUPPORTING INFORMATION

Additional Supporting Information may be found in the online version of this article at the publisher's web-site:

Table S1. Sequence of each oligomer set for preparing genotype panel oligomers.

Table S2. Sequence of each genotype panel oligomers.

Table S3. Validation of our sample using current NAT system.

Table S4. Summary of DLC-chip analysis of genotype panels and international standards.

JAPANESE DERMATOLOGICAL ASSOCIATION
THE JOURNAL OF DERMATOLOGY

doi: 10.1111/1346-8138.12374 *Journal of Dermatology* 2014; **41**: 26–28

MEETING REPORT

Meeting report on the possible proposal of an extranodal primary cutaneous variant in the lymphoma type of adult T-cell leukemia-lymphoma

Kunihiro TSUKASAKI,[1] Yositaka IMAIZUMI,[2] Yoshiki TOKURA,[3] Kouichi OHSHIMA,[4] Kazuhiro KAWAI,[5,6] Atae UTSUNOMIYA,[7] Masahiro AMANO,[8] Toshiki WATANABE,[9] Shigeo NAKAMURA,[10] Keiji IWATSUKI,[11] Shimeru KAMIHIRA,[12] Kazunari YAMAGUCHI,[13] Masanori SHIMOYAMA[14]

[1]Department of Hematology, National Cancer Center Hospital East, Kashiwa, [2]Department of Hematology, Atomic Bomb Disease and Hibakusha Medicine Unit, Atomic Bomb Disease Institute, Nagasaki University, Nagasaki, [3]Department of Dermatology, Hamamatsu University School of Medicine, Hamamatsu, [4]Department of Pathology, Kurume University, Kurume, [5]Department of Dermatology, Kido Hospital, Niigata, [6]Department of Dermatology, Kagoshima University Graduate School of Medical and Dental Sciences, Kagoshima, [7]Department of Hematology, Imamura Bun-in Hospital, Kagoshima, [8]Department of Dermatology, Miyazaki University, Miyazaki, [9]Graduate School of Frontier Sciences, The University of Tokyo, Tokyo, [10]Pathology and Laboratory Medicine, Nagoya University Hospital, Nagoya, [11]Department of Dermatology, Okayama University Graduate School of Medicine, Okayama, [12]Laboratory Medicine, Nagasaki Minato Medical Center, Nagasaki, [13]Cell Modulation, Institute of Molecular Embryology and Genetics, Kumamoto University, Kumamoto, and [14]Multicenter Institutional Clinical Trial Support Center, National Cancer Center, Tokyo, Japan

ABSTRACT

Based on the advances in research on the clinicopathophysiology of adult T-cell leukemia-lymphoma (ATL), Japanese researchers collected and evaluated cases of smoldering ATL exhibiting primary cutaneous manifestation but showing poor prognosis. Macroscopic findings of skin eruptions were categorized into the patch, plaque, multipapular, nodulotumoral, erythrodermic and purpuric types, as previously reported. Pathological findings were divided into low or high grade based on epidermotropism, tumor cell size and perivascular infiltration. Eight eligible cases were evaluated among 14 collected cases. Macroscopic findings were nodulotumoral in six cases, a subcutaneous tumor in one case and plaque in one case, and the number and size were heterogeneous in each case. Pathological findings of all eight cases were T-cell lymphoma, high-grade type (pleomorphic, medium or large size), with prominent perivascular infiltration and scant epidermotropism. To diagnose such cases as the "lymphoma type of ATL, extranodal primary cutaneous variant", it is essential to examine each case carefully, including cutaneous lesions at onset, lymph nodes and other organ involvement using computed tomography (CT) and/or positron emission tomography/CT, as well as the percentage of abnormal lymphocytes in peripheral blood. Based on the results of an ongoing nationwide survey on ATL, ATL with cutaneous lesions will be analyzed to investigate the incidence and prognosis of the so-called "lymphoma type of ATL, extranodal primary cutaneous variant".

Key words: adult T-cell leukemia/lymphoma, extranodal primary cutaneous variant, lymphoma type adult T-cell leukemia/lymphoma, smoldering adult T-cell leukemia/lymphoma.

PURPOSE OF THE MEETING

On the basis of the modes of initial presentation and natural history of patients with adult T-cell leukemia/lymphoma (ATL), the four clinical subtypes of acute, lymphoma, chronic and smoldering have been recognized. Diagnostic criteria for the clinical subtypes were proposed[1] and significant prognostic factors were determined in 1991.[2] Since then, patients with ATL were stratified into two groups, aggressive ones consisting of acute, lymphoma and unfavorable chronic types, and indolent ones consisting of favorable chronic and smoldering types, in which the chronic type was further divided into favorable

Correspondence: Kunihiro Tsukasaki, M.D., Ph.D., Department of Hematology, National Cancer Center Hospital East, 6-5-1 Kashiwanoha, Kashiwa-shi, Chiba 277-8577, Japan. Email: ktsukasa@east.ncc.go.jp
Received 29 October 2013; accepted 4 November 2013.

and unfavorable according to significant prognostic factors. This stratification was useful for the selection of treatment, in which most patients with aggressive forms were treated with systemic chemotherapy, while those with indolent forms underwent watchful waiting or local therapy only.

In the clinical subtype classification, however, the lymphoma type did not include extranodal variants because of the rarity of such cases at that time. Since then, variants of extranodal lymphoma type such as primary cutaneous ATL and primary gastrointestinal ATL have been reported. The extranodal primary cutaneous variant included in smoldering type made it particularly difficult for physicians to choose the initial treatment.[3–6] Furthermore, the extranodal primary gastrointestinal variant included in the acute type was reported to respond to treatment and be associated with long-term survival. On the contrary, the localized lymphoma type, which was rare in the initial survey in Japan, was reported to consist of approximately 10% of acute and lymphoma types of ATL, and was associated with relatively favorable prognosis after chemotherapy in a recent nationwide survey in Japan.[7]

Based on the advances in research on the clinicopathophysiology of ATL as described above, Japanese researchers, focusing on ATL, joined by the support of a grant (H23-gan rinsho-ippan-022), collected and evaluated cases such as of the localized lymphoma type and extranodal variants originating from several organs to reconsider the subclassification for the appropriate selection of treatment.

This research group, consisting of Japanese hematologists, dermatologists, pathologists, epidemiologists and oncovirologists, aimed at collecting cases as follows: smoldering type with primary cutaneous manifestation resulting in poor prognosis, acute type with the manifestation of an extranodal variant of primary gastrointestinal or nasopharyngeal type, and localized lymphoma type, reviewing clinicopathological findings and proposing the consensus report.

This report summarizes the discussion of the first meeting on this project, focusing on the extranodal primary cutaneous variant.

ELIGIBILITY CRITERIA OF PATIENTS FOR THE EVALUATION

Eligibility criteria included smoldering ATL with only cutaneous lesions confirmed by histopathology, and with survival after diagnosis of less than 1 year as a rule but less than 3 years being allowed. Each dermatologist/hematologist picked up the cases, and filled out the case report forms with macro-photographs and histological specimens of cutaneous lesions. We categorized the macroscopic findings of skin eruptions into the patch, plaque, multipapular, nodulotumoral, erythrodermic and purpuric types, as previously reported.[6] When multiple types of skin eruption exist in a patient, the most severe type should be described if a consensus on the hierarchy of severity in the types exists: patch and plaque were considered the lowest and second lowest severity, respectively, and nodulotumoral was most severe. There was no consensus on multipapular, erythrodermic and purpuric types, but multipapular and purpuric types were considered intermediate between nodulotumoral and plaque, and should be described separately. Erythrodermic type should still be carefully evaluated. Subcutaneous tumors were specified but included as the nodulotumoral type.

Pathological findings were divided into low or high grade based on epidermotropism, the cell size and perivascular infiltration.[3]

RESULTS

Fourteen cases were evaluated, but six of them were deemed ineligible because of the period from the onset of cutaneous lesions to the diagnosis of ATL being more than 4 months in five cases and concurrent lymph node lesions at onset not indicating the smoldering but acute type in one case. Case reports were provided by Dr Y. Sawada (University of Occupational and Environmental Health, Fukuoka), Dr Y. Uchida (Kagoshima University, Kagoshima), Dr T. Johno (Kumamoto University, Kumamoto), Dr M. Takenaka (Nagasaki University, Nagasaki), Dr K. Uchimaru (Tokyo University, Tokyo) and Dr K. Tobinai (National Cancer Center Hospital, Tokyo).

All of the eight eligible cases were diagnosed as smoldering ATL. Macroscopic findings were nodulotumoral in six cases, a subcutaneous tumor in one case and plaque in one case, and the number and size were heterogeneous in each case. Pathological findings of all eight cases were consistent with T-cell lymphoma, high-grade type (pleomorphic, medium or large size), with prominent perivascular infiltration and scant epidermotropism. Median times from the diagnosis to acute crisis, and onset of the cutaneous lesion to acute crisis, were 6 and 7 months, respectively (data not shown).

DISCUSSION (PROBLEMS AND TO-DO LIST)

Accurate evaluation is essential at onset: cutaneous lesion at onset, lymph nodes and other organ involvement using computed tomography (CT) and/or positron emission tomography (PET)/CT, as well as the percentage of abnormal lymphocytes in peripheral blood (PB).

The clinical course of each lesion including cutaneous lesions should be evaluated with respect to the timing of diagnosis. As for the "extranodal primary cutaneous variant", further case evaluation is essential, including those with a relatively favorable prognosis.

As for the pathological diagnosis of cutaneous lesions, the biopsy site including macroscopic findings should be described. It is possible that specimens were biopsied at sites with a poor prognostic hierarchy in this case series.

In general, pathological findings of cutaneous lesion of ATL appear to be epidermotropic and non-epidermotropic. All of the cases in this meeting were high-grade peripheral T-cell lymphoma (PTCL)-like, and no case was low-grade cutaneous T-cell lymphoma-like because cases with a poor prognosis were collected.

Seven out of eight eligible cases were the "extranodal primary cutaneous variant", consisting of six cases of nodulotu-

moral and one of plaque macroscopically, and all seven were high-grade PTCL microscopically. The remaining one was described as a "primary subcutaneous tumor". There was a comment against the "primary subcutaneous tumor" type included in the "primary cutaneous variant".

To diagnose such cases as the "lymphoma type of ATL, extranodal primary cutaneous variant", it is essential to examine each case carefully, including cutaneous lesions at onset, lymph nodes and other organ involvement using CT and/or PET/CT, as well as the percentage of abnormal lymphocytes in PB (Appendix 1).

The application of clinical staging based on the extension of cutaneous lesions requires further investigation.

Some ATL patients with multipapular type cutaneous lesions were reported to show a rapidly progressive clinical course.[6] Such cases should also be collected and analyzed.

FUTURE PLAN

More cases should be collected and investigated.

Based on the results of an ongoing nationwide survey on ATL, ATL with cutaneous lesions will be analyzed to investigate the incidence and prognosis of the so-called the "lymphoma type of ATL, extranodal primary cutaneous variant".

ACKNOWLEDGMENT: This work was supported by a grant for cancer research (H23-gan rinsho-ippan-022) from the Ministry of Health, Labor and Welfare in Japan.

CONFLICT OF INTEREST: None.

REFERENCES

1 Shimoyama M, Members of the Lymphoma Study Group (1984–87). Diagnostic criteria and classification of clinical subtypes of adult T-cell leukaemia-lymphoma: a report from the Lymphoma Study Group (1984–87). *Br J Haematol* 1991; **79**: 428–437.

2 Lymphoma Study Group (1984–87). Major prognostic factors of patients with adult T-cell leukemia-lymphoma: a cooperative study. *Leuk Res* 1991; **15**: 81–90.

3 Ohshima K, Jaffe ES, Kikuchi M. Adult T-cell leukemia/lymphoma, In: Swerdlow SH, Campo E, Harris NL, eds. *WHO Classification of Tumour of Haemaopoietic and Lymphoid Tissues*. 4th edn. Lyon: IARC Press, 2008; 281–284.

4 Bittencourt AL, da Graças Vieira M, Brites CR, Farre L, Barbosa HS. Adult T-cell leukemia/lymphoma in Bahia, Brazil: analysis of prognostic factors in a group of 70 patients. *Am J Clin Pathol* 2007; **128**: 875–882.

5 Amano M, Kurokawa M, Ogata K *et al.* New entity, definition and diagnostic criteria of cutaneous adult T-cell leukemia/lymphoma: human T-lymphotropic virus type 1 proviral DNA load can distinguish between cutaneous and smoldering types. *J Dermatol* 2008; **35**(5): 270–275.

6 Sawada Y, Hino R, Hama K *et al.* Type of skin eruption is an independent prognostic indicator for adult T-cell leukemia/lymphoma. *Blood* 2011; **117**(15): 3961–3967.

7 Katsuya H, Yamanaka T, Ishitsuka K *et al.* Prognostic index for acute- and lymphoma-type adult T-cell leukemia/lymphoma. *J Clin Oncol* 2012; **30**(14): 1635–1640.

APPENDIX I

For the diagnostic criteria of the lymphoma type of the extranodal primary cutaneous variant, no definite appearance of abnormal cells in PB (≤1%) is essential.

Evaluation of abnormal lymphocytes by flow cytometry as well as based on the morphology is warranted to calculate the cells as a real number. However, such criteria are quite different from the original criteria for the definition of ATL and clinical subtype classification of ATL. Therefore, such a proposal requires careful analyses and evaluation. Discussion on this issue is currently limited in this meeting.

For ATL, quantitative evaluation of cutaneous lesions such as using the modified Severity Weighted Assessment Tool should be investigated; however, it is not easily applicable.

Macroscopic findings of cutaneous lesions are a significant prognostic factor in ATL. However, the combination of other parameters, for example, tumor markers such as lactate dehydrogenase and soluble IL-2 receptor, needs to be investigated.

Cancer Science
The official journal of the Japanese Cancer Association

Adult T-cell leukemia cells are characterized by abnormalities of *Helios* expression that promote T cell growth

Satomi Asanuma,[1] Makoto Yamagishi,[1] Katsuaki Kawanami,[1] Kazumi Nakano,[1] Aiko Sato-Otsubo,[2] Satsuki Muto,[2] Masashi Sanada,[2] Tadanori Yamochi,[1] Seiichiro Kobayashi,[3] Atae Utsunomiya,[4] Masako Iwanaga,[5] Kazunari Yamaguchi,[6] Kaoru Uchimaru,[3] Seishi Ogawa[2] and Toshiki Watanabe[1,7]

[1]Graduate School of Frontier Sciences, The University of Tokyo; [2]Cancer Genomics Project, Graduate School of Medicine, The University of Tokyo; [3]Institute of Medical Science, The University of Tokyo, Tokyo; [4]Department of Hematology, Imamura Bun-in Hospital, Kagoshima; [5]Graduate School of Public Health, Teikyo University; [6]Department of Safety Research on Blood and Biological Products, National Institute of Infectious Diseases, Tokyo, Japan

(Received December 27, 2012/Revised April 11, 2013/Accepted April 15, 2013/Accepted manuscript online April 18, 2013/Article first published online May 19, 2013)

Molecular abnormalities involved in the multistep leukemogenesis of adult T-cell leukemia (ATL) remain to be clarified. Based on our integrated database, we focused on the expression patterns and levels of Ikaros family genes, *Ikaros*, *Helios*, and *Aiolos*, in ATL patients and HTLV-1 carriers. The results revealed profound deregulation of Helios expression, a pivotal regulator in the control of T-cell differentiation and activation. The majority of ATL samples (32/37 cases) showed abnormal splicing of Helios expression, and four cases did not express Helios. In addition, novel genomic loss in *Helios* locus was observed in 17/168 cases. We identified four ATL-specific short Helios isoforms and revealed their dominant-negative function. Ectopic expression of ATL-type Helios isoform as well as knockdown of normal Helios or Ikaros promoted T-cell growth. Global mRNA profiling and pathway analysis showed activation of several signaling pathways important for lymphocyte proliferation and survival. These data provide new insights into the molecular involvement of Helios function in the leukemogenesis and phenotype of ATL cells, indicating that Helios deregulation is one of the novel molecular hallmarks of ATL. (*Cancer Sci* 2013; 104: 1097–1106)

Adult T-cell leukemia (ATL) is a highly aggressive malignancy of mature CD4+ T cells and is caused by HTLV-1. After HTLV-1 infection, ATL is thought to develop following a multitude of events, including both genetic and epigenetic changes in the cells. Although many aspects of HTLV-1 biology have been elucidated, the detailed molecular mechanism of ATL leukemogenesis remains largely unknown.[1,2] Therefore, to precisely define the comprehensive abnormalities associated with ATL leukemogenesis, we previously carried out global mRNA and miRNA profiling of ATL cells derived from a large number of patients.[3,4] In this study, we focused on Ikaros family genes, especially Helios, on the basis of our integrated profiling of expression and gene copy number in ATL cells, which revealed the deregulated expression of this family of genes and genomic loss of *Helios* locus.

Ikaros family genes are specifically expressed in the hematopoietic system and play a vital role in regulation of lymphoid development and differentiation.[5–11] In addition, they are known to function as tumor suppressors during leukemogenesis according to several genetic studies carried out in mouse models.[12–15] Recently, many studies reported the deregulated splicing of Ikaros and the deletion of *Ikaros* locus in several human leukemias.[16–23] These abnormalities are associated with poor prognoses.[24–27] Helios is mainly expressed in the T-cell lineage.[10,11] Genomic changes and abnormal expression of Helios are also observed in some patients with T-cell malignancies.[18,28–31] However, in contrast to Ikaros, the substantial impact of aberrant Helios expression remains to be elucidated because of the absence of functional information, including the target genes of Helios.

In this study, we carried out a detailed expression analysis of Ikaros family genes in a large panel of clinical samples from ATL patients and HTLV-1 carriers and consequently identified a novel molecular characteristic, that is, abnormal splicing of Helios and loss of expression, which seems to be a significant key factor in leukemogenesis affecting the regulation of T-cell proliferation.

Materials and Methods

Cell lines and clinical samples. HeLa and 293T cells were cultivated in DMEM supplemented with 10% FCS. Human leukemic T cells, Jurkat, Molt-4, and CEM, ATL-derived, MT-1 and TL-Om1, and HTLV-1-infected MT-2 and Hut-102 cell lines were all maintained in RPMI-1640 with 10% FCS. The PBMCs from ATL patients of four clinical subtypes[32] and healthy volunteers were a part of those collected with informed consent as a collaborative project of the Joint Study on Prognostic Factors of ATL Development. The project was approved by the Institute of Medical Sciences, University of Tokyo Human Genome Research Ethics Committee (Tokyo, Japan). Clinical information of ATL individuals is provided in Table S1.

RNA isolation and RT-PCR analysis. The preparation of total RNA and synthesis of the first strand of cDNA were described previously.[3] The mRNAs of Ikaros family genes were examined by PCR with Platinum Taq DNA Polymerase High Fidelity (Invitrogen, Carlsbad, CA, USA). The PCR products were sequenced by automated DNA sequencer. Nested PCR amplification was carried out with diluted full-length PCR products by Accuprime Taq DNA polymerase High Fidelity (Invitrogen). Quantitative PCR was carried out as previously described.[3] The specific primer sets for each PCR are described in Table S2.

Immunoblot analysis. Cells were collected, washed with PBS, and lysed with RIPA buffer. For immunoprecipitation, cells were lysed with TNE buffer and incubated with specific antibody. Proteins samples were then analyzed by immunoblots with specific antibodies: anti-tubulin, anti-Ikaros, and anti-Helios antibodies were from Santa Cruz Biotechnology (Santa Cruz, CA, USA). Mouse anti-FLAG antibody (M2) was from Sigma-Aldrich (St. Louis, MO, USA). Rabbit polyclonal anti-HA

[7]To whom correspondence should be addressed.
E-mail: tnabe@ims.u-tokyo.ac.jp

doi: 10.1111/cas.12181

antibody was from MBL (Nagoya, Japan). Anti-mouse, rabbit, and goat secondary antibodies were from Promega (Fitchburg, WI, USA).

Immunostaining. HeLa cells were cultured on coverslip slides and transfected with the indicated expression vectors by Lipofectamine LTX (Invitrogen). At 24 h post transfection, cells were washed three times with PBS, fixed in 4% paraformaldehyde, and permeabilized with 0.1% Triton X-100. Then, cells were stained with primary antibodies (diluted 1:500 to 1:2000). Alexa-488 or 546-conjugated secondary antibodies (Molecular Probes, Life Technologies, Carlsbad, CA, USA) were used for detection of specific targets, and DAPI was used for nuclear staining. Images were acquired by using a Nikon A1 confocal microscope (Nikon, Tokyo, Japan).

Electrophoretic mobility-shift assay. Experimental conditions and detail methods were previously reported.[3] For evaluation of DNA binding activity, 3–5 μg nuclear extracts from each transfectant were used per each lane of electrophoresis. The oligonucleotide sequences used as a probe are provided in Table S2.

Luciferase assay. The pGL4.10-firefly vector (Promega) containing *Hes1* promoter was used as a reporter vector and RSV-renilla vector was used as a control vector. HeLa cells were transiently transfected with these reporters and each Ikaros or/and Helios expression vector by Lipofectamine 2000 reagent (Invitrogen). The luciferase activities were quantified by the Dual-Luciferase Reporter Assay System (Promega) at 24 h post-transfection.

Retroviral construction and transduction. The FLAG-Hel-5 cDNA sequence was subcloned into retrovirus vector pRx-puro. Stable cell populations expressing Hel-5 were selected by puromycin. The shRNA-expressing retroviral vectors and virus production procedures have been established.[3] The shRNA sequences are listed in Table S2. Stable cell populations were obtained by puromycin or G418 selection.

Proliferation assays. Cells (0.5 or 1.0×10^4) were plated in 96-well plates with media supplemented with 10% or 0.2% FCS. The cell numbers were evaluated for 4 days by Cell Counting Kit-8 (Dojindo, Kumamoto, Japan). The averages of at least three independent experiments are shown.

Gene expression microarray analyses. Gene expression microarray used the 4 × 44K Whole Human Genome Oligo Microarray (Agilent Technologies, Santa Clara, CA, USA); detailed methods were previously reported.[3] Coordinates have been deposited in the Gene Expression Omnibus database with accession numbers GSE33615 (gene expression microarray), GSE33602 (copy number analyses), and GSE41796 (Jurkat models).

Results

Abnormal expression of short Helios transcripts in primary ATL cells. To characterize the gene expression signature in primary ATL cells, we previously carried out mRNA microarray analyses on a large number of samples. The comprehensive survey unveiled deregulated expression of Ikaros family genes; transcription levels of Ikaros and Aiolos were downregulated in ATL samples, whereas Helios was upregulated (Fig. S1). Thus, we examined the detailed expression patterns and levels of Ikaros family members in PBMCs derived from a panel of ATL patients and HTLV-1 carriers (Fig. 1a). Compared with control PBMCs from normal volunteers (Fig. 1b), the expression levels of Ikaros and Aiolos seemed to be downregulated in ATL samples, consistent with our microarray results. However, there were obvious abnormalities in the expression patterns of Helios. The main isoform of Helios was changed from full-length Hel-1 to Hel-2, which lacks exon 3 that contains the first N-terminal zinc finger in the DNA-binding domain. In addition, four ATL-specific Helios short transcripts were identified (Fig. 1c). Among them, Hel-5 and Hel-6 have been reported to be expressed in ATL.[29] We also identified two novel variants, Hel-v1 that lacks exons 3 and 4 and Hel-v2 that lacks exons 2, 3, and 6. These abnormal Helios variants were also expressed in the samples of high-risk HTLV-1 carriers, who subsequently developed ATL in the next few years. Furthermore, nested PCR revealed that Hel-5 or Hel-6 were expressed in a majority of ATL samples (17/22 acute cases, 10/10 chronic cases, and 5/5 smoldering cases; total, 32/37 cases) (Fig. 1d, upper panels), whereas Hel-v1 was expressed only in limited cases of ATL (Fig. 1d, lower panels). In four cases, Helios was not expressed. Collectively, our mRNA analysis showed that Helios expression was generally deregulated in ATL cells.

Genomic abnormalities at the *Helios* locus in primary ATL cells. To investigate the *Helios* locus in ATL, we retrieved data from our gene copy number analysis[3] and found that specific genomic deletion was accumulated at the *Helios* locus in ATL samples (17/168 cases, Fig. 2). All 17 cases were aggressive-type ATL (12/17 lymphoma types and 5/17 acute types). Furthermore, we found that two acute ATL cases in Figure 1(a) (#9 and #14), which showed severely deregulated or lost Helios expression, had a genomic deletion of the *Helios* locus.

Dimerization ability of ATL-type Helios isoforms with wild-type Helios or Ikaros. Consistent with a previously published report,[33] co-immunoprecipitation analyses confirmed that wild-type Hel-1 formed homodimers with themselves and heterodimers with wild-type Ikaros (Ik-1) protein (Fig. 3a, top panel, lane 1 and lane 4). In contrast, the dimerization activity of another artificial Helios mutant (Hel-ΔC), which lacks the dimerization domain at the C-terminal region, was dramatically declined (Fig. 3b, top panel, lane 1 and lane 4). We confirmed that all ATL-type Helios proteins could interact with Hel-1 and Ik-1, despite the fact that all of them lack various sets of the N-terminal exons (Fig. 3c–f).

Cytoplasmic localization of ATL-type Helios isoforms lacking exon 6. Ectopically expressed Hel-1 and Ik-1 were localized in the nucleus (Fig. 4a, top two panels). Regarding the ATL-type Helios isoforms, we found that Hel-5 and Hel-v1 were localized in the nucleus, whereas Hel-6 and Hel-v2, both of which lack exon 6, were substantially localized in the cytoplasm (Fig. 4a, middle four panels). We also confirmed the cytoplasmic localization of Hel-Δexon 6, which is an artificial Helios mutant lacking only exon 6 (Fig. 4a, bottom panel). Thus, exon 6 appears to be critical for nuclear localization of Helios proteins. Furthermore, defect of exon 6 led to disruption of the

Fig. 1. (On the next page) Abnormal expression of Helios mRNA in primary adult T-cell leukemia (ATL) cells. (a) Expression analysis of Ikaros family genes in PBMCs by full-length RT-PCR (Acute, $n = 22$; Chronic, $n = 10$; Smoldering, $n = 5$; HTLV-1 carriers, $n = 5$; High-risk carriers, $n = 4$). To detect and distinguish alternative splicing variants, PCR analyses were carried out with the sense and antisense primer sets designed in the first and final exons of each full-length transcript of Ikaros family genes. Obtained cDNAs were cloned and their sequences were analyzed. The samples acute #4, 4′, and 4″ were derived from the same patient, but were studied independently. (b) Expression of Ikaros family genes in PBMCs from normal volunteers ($n = 10$). (c) Schematic representation of Hel-1, Hel-2, and ATL-type Helios isoforms identified in this study. Hel-variant 1 (Hel-v1) and Hel-variant 2 (Hel-v2) are novel isoforms in ATL. Arrows indicate primer locations of full-length PCR for Helios. Ex, exon; F1–F6, functional zinc-finger domains. (d) Nested PCR with specific primer sets, which were designed at exon junction of exon 1–5 or exon 2–5 for detection of Hel-5 and Hel-6 (upper panel), or detection of Hel-v1 (lower panel), respectively. Arrows indicate primer locations.

doi: 10.1111/cas.12181

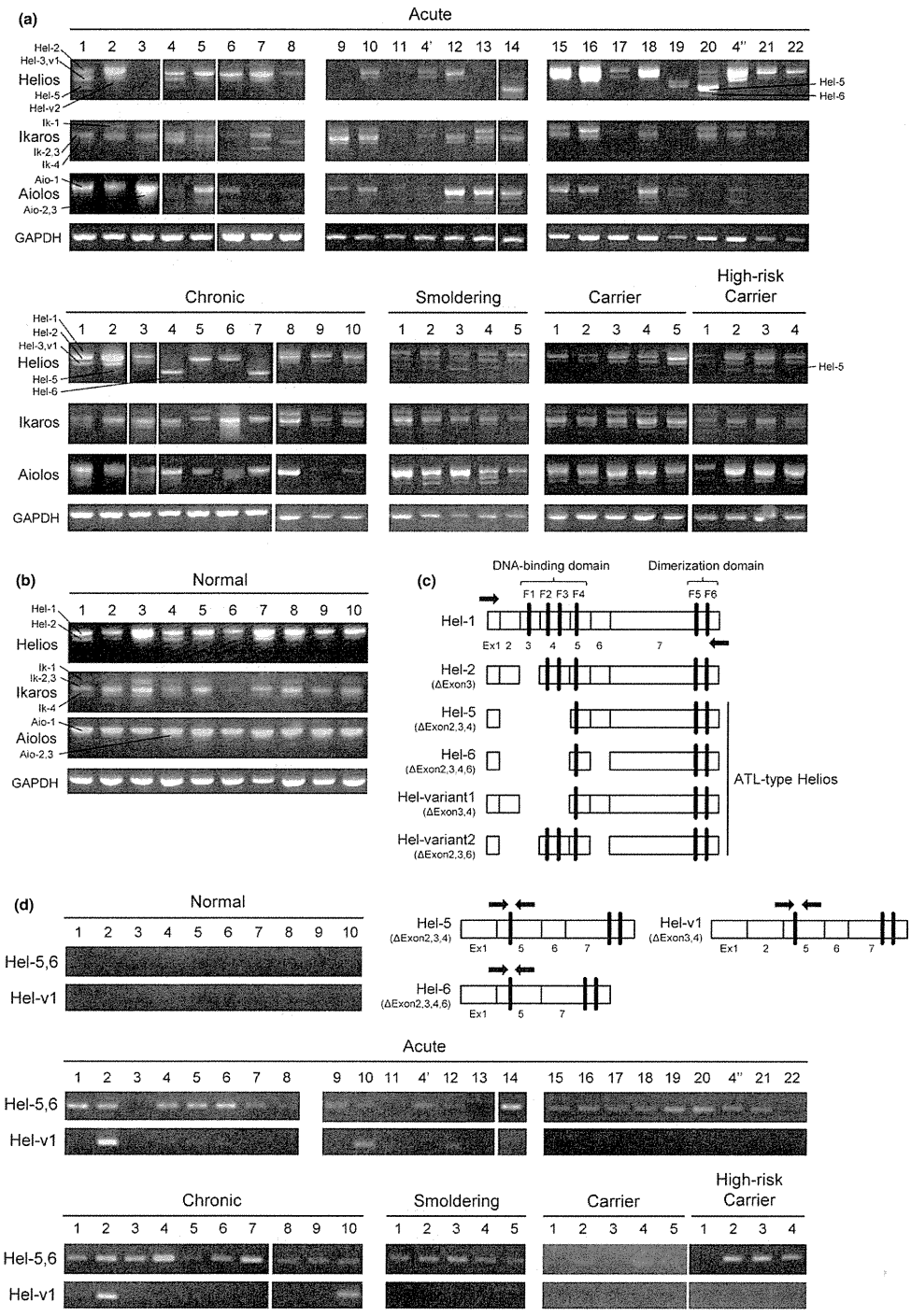

cellular localization of binding partners. When Hel-6 or Hel-v2 were co-expressed with Hel-1 or Ik-1, they were co-localized in the cytoplasm (Fig. 4b, Fig. S2).

Dominant-negative function of ATL-type Helios isoforms against wild-type Helios and Ikaros. We next examined the functional aspects of these ATL-type Helios isoforms by evaluating their DNA-binding capacities. For EMSA, we used an oligonucleotide probe derived from the promoter region of human *Hes1*, which was a direct target of Ikaros.[34,35] Ectopically expressed Hel-1 or Ik-1 could bind human *Hes1* promoter DNA (Fig. 5a). Supershift assays confirmed the binding specificity (Fig. 5b). In contrast, all ATL-type Helios isoforms did not show any specific binding to the *Hes1* promoter (Fig. 5a). This impossibility of specific DNA binding of ATL-type Helios was confirmed with another independent DNA probe, IkBS4[33,36] (data not shown). In addition, it was found in co-expression experiments that Hel-5 had antagonistic effects on the DNA binding capacity of Ik-1 in a dose-dependent manner (Fig. 5c). Reporter assays showed that Hel-1 and Ik-1 suppressed *Hes1* promoter activity. However, ATL-type Helios isoforms did not show any suppressive activity, and actually slightly activated the promoter (Fig. 5d). Furthermore, they also inhibited the suppressive function of Hel-1 and Ik-1 in a dose-dependent manner (Fig. 5e, Fig. S3). These data clearly indicate that ATL-type Helios isoforms are functionally defective because of a DNA binding deficiency and act dominant-negatively in transcriptional suppression induced by Hel-1 or Ik-1. We also confirmed that Hel-2, which lacks only exon 3 and is a major isoform in ATL cells, did not possess suppressive activity against *Hes1* promoter in spite of having binding activity (Fig. 5a,d).

Major ATL-type Helios variant, Hel-5, promotes T cell growth. Given the tumor-suppressive roles of Ikaros family members,[12–15] it was expected that abnormal splicing of Helios could contribute to T cell leukemogenesis. The mRNA level of Helios was significantly downregulated in ATL-related cell lines compared with that in T-cell lines without HTLV-1 (Fig. 6a, Fig. S4). Moreover, Helios protein was not detected in any ATL-derived or HTLV-1-infected cell lines used in this study (Fig. 6b). In contrast, the expression levels of Ikaros mRNA did not show major differences between HTLV-1-infected and uninfected T-cell lines. Those of Aiolos were low in most cell lines irrespective of HTLV-1 infection (Fig. 6a, Fig. S4). Ikaros protein was detected in all T-cell lines used in this study (Fig. 6b). To elucidate the cellular effects of the expression of dominant-negative ATL-type Helios isoforms in T cells, we established stable Jurkat cells expressing Hel-5 (Fig. 6c). A cell proliferation assay confirmed that Hel-5 expression significantly promoted Jurkat cell proliferation

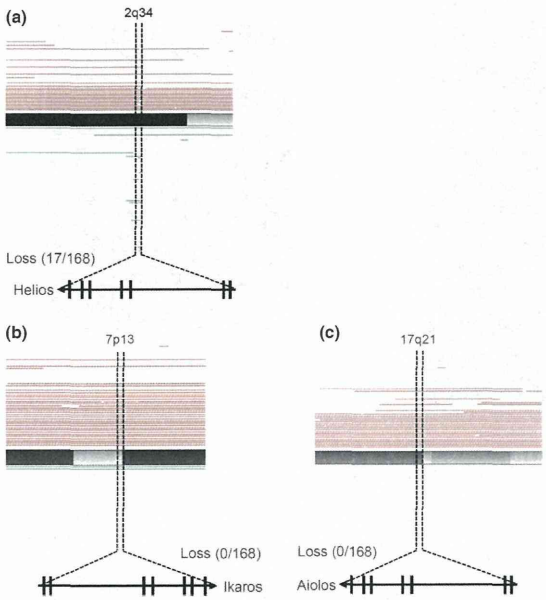

Fig. 2. Genetic abnormalities in *Helios* locus in primary adult T-cell leukemia cells. The results of our copy number analyses[3] (total number, $n = 168$; acute type, $n = 35$; chronic type, $n = 41$; lymphoma type, $n = 44$; smoldering type, $n = 10$; intermediate, $n = 1$; unknown diagnosis, $n = 37$). Tumor-associated deletion of *Helios* region (17/168) was detected (a). No specific genomic losses were observed in *Ikaros* (b) or *Aiolos* loci (c). Recurrent genetic changes are depicted by horizontal lines based on Copy Number Analyser for GeneChip output of the single nucleotide polymorphism array analysis.

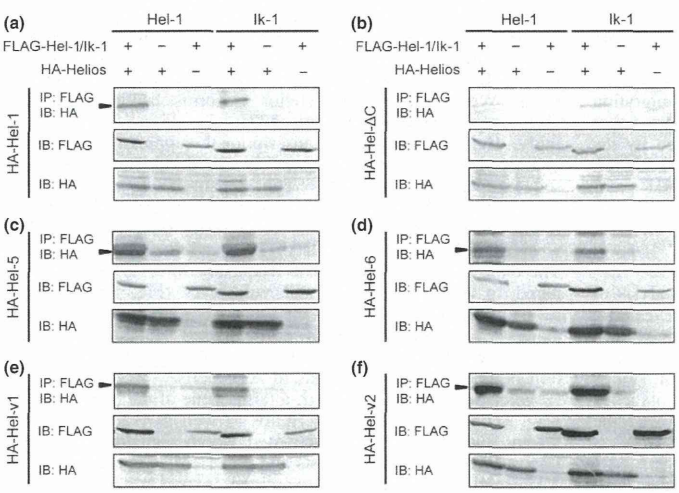

Fig. 3. Dimerization ability of adult T-cell leukemia (ATL)-type Helios isoforms. *In vitro* dimerization assays by co-immunoprecipitation between ATL-type Helios and wild-type Helios or Ikaros proteins. 293T cells were transfected with the indicated combination of expression vectors and subjected to co-immunoprecipitation analyses (top panels). Arrowheads indicate the complex of FLAG and HA-tagged proteins. Middle and bottom panels show the input samples. Hel-1 (a) and Hel-ΔC (b) included as positive and negative controls, respectively. ATL-specific isoforms, Hel-5 (c), Hel-6 (d), Hel-v1 (e), and Hel-v2 (f) were tested. IB, immunoblot; IP, immunoprecipitant.

doi: 10.1111/cas.12181

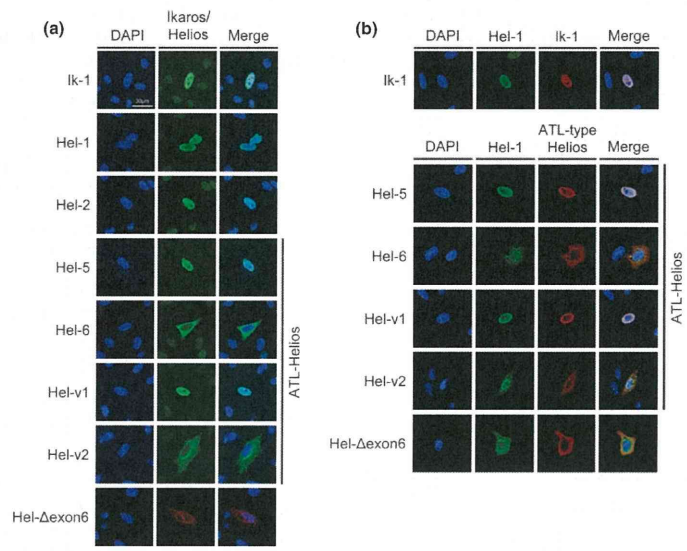

Fig. 4. Subcellular localization of adult T-cell leukemia (ATL)-type Helios isoforms. Immunostaining analyses of Helios and Ikaros proteins. HeLa cells were transfected with each individual expression vector (a) or the indicated combination of expression vectors (b). Each protein was visualized with anti-FLAG (green) or anti-HA antibodies (red). Nuclei were detected by DAPI staining (blue). Colocalization between Ik-1 and ATL-type Helios was shown in Fig. S2. Hel-v1, Hel-variant 1; Hel-v2, Hel-variant 2.

(Fig. 6d). To examine whether the cellular effect of Hel-5 was due to its dominant-negative function against Hel-1 and Ik-1, we carried out further knockdown analyses with specific shRNAs (Fig. 6e). The results showed that knockdown of wild-type Helios or Ikaros led to enhanced cell growth (Fig. 6f), which was consistent with the results of enforced Hel-5 expression. These results collectively suggested that counteraction of Ikaros or Helios by dominant-negative isoforms contributed to T cell growth.

Helios deficiency causes expression of various genes in T cells. We globally searched mRNA expression changes using microarray analysis of Jurkat cells expressing Hel-5 and those of knocked-down Helios or Ikaros (Fig. 7a,b). The results clearly showed differentially expressed gene sets between the transformants and control cells (Fig. 7c). Furthermore, pathway analysis[37] of each upregulated gene set identified activation of several signaling cascades. In particular, we focused on six common pathways identified in both Hel-5 transduced and Helios or Ikaros knocked-down Jurkat cells (Fig. 7d). These pathways are important for various T cell regulations, for example, cell growth, apoptosis resistance, and migration activity. Among these pathways, it has not been reported that the shingosine-1-phosphate (S1P) pathway is regulated by the Ikaros family. We confirmed overexpressed *S1PR1* and *S1PR3*, which are critical receptors for the activation of the S1P pathway, in manipulated Jurkat samples (Fig. 7e).

Discussion

In the present study, on the basis of the integrated analysis of ATL cells using our biomaterial bank in Japan, we revealed a novel molecular characteristic of ATL cells, which is a profound abnormality in the expression of Helios. The abnormal alternative splicing and, in some cases, loss of Helios expression appear to be a part of the basis for advantageous cell growth and survival in ATL cells. We also showed the tumor-suppressive function and target genes, as well as pathways of Helios, in mature human T cells.

Characterization of Ikaros family members revealed profound abnormalities in Helios expression in ATL cells: (i) biased and increased expression of alternatively spliced variants; (ii) suppression of Hel-1 expression; (iii) lack of Helios expression in some cases; and (iv) frequent genomic defects of the *Helios* locus. Our results also revealed that alternatively spliced Helios variants are expressed in PBMCs of HTLV-1 carriers, suggesting that the abnormal splicing of Helios may occur in HTLV-1-infected cells at the carrier state until progression to leukemia development. However, the genomic deletions appear to be one of the important genetic events during the latter stages of leukemia development, as they were observed only in aggressive subtypes of ATL.

The structural characteristics of the ATL-type Helios variants involve a selective lack of one or more zinc fingers in the N-terminal domain. The results of this study indicated that these variant proteins lost DNA binding activity, whereas the capacity of dimerization was preserved. Therefore, these variant proteins hindered transcriptional activities of Ikaros family proteins, showing dominant-negative effects. In addition, a part of ATL-type Helios isoform, which lacks exon 6, is linked to abnormal localization of wild-type Helios and Ikaros. We confirmed that Helios isoforms lacking exon 6 were overexpressed in primary ATL cells (Fig. S5). Interestingly, Hel-2 has reduced transcriptional suppressive activity compared with Hel-1, although it can bind to the target sequence as well as Hel-1. This is similar to a previous report,[36] which noted that the activity of mouse Ik-2 protein for the reporter gene was remarkably lower than that of Ik-1, whereas the binding affinities of Ik-1 and Ik-2 were similar. The exon 3 skip occurred more frequently in ATL cells, compared to PBMCs from normal volunteers (Fig. S6). These results collectively indicate that all abnormalities of Helios expression, including loss of or decreased Hel-1 expression and upregulated Hel-2 and ATL-type Helios, result in abrogation of Ikaros family functions in ATL cells.

We also confirmed that *Hes1*, a target gene of the Notch pathway, is one of the targets of Helios as well as Ikaros.[34,35] A recent study reported that activated Notch signaling may be important to ATL pathogenesis and that Hes1 is upregulated in ATL cells.[38] Thus, we examined expression levels of Hes1 mRNA by quantitative RT-PCR and confirmed the

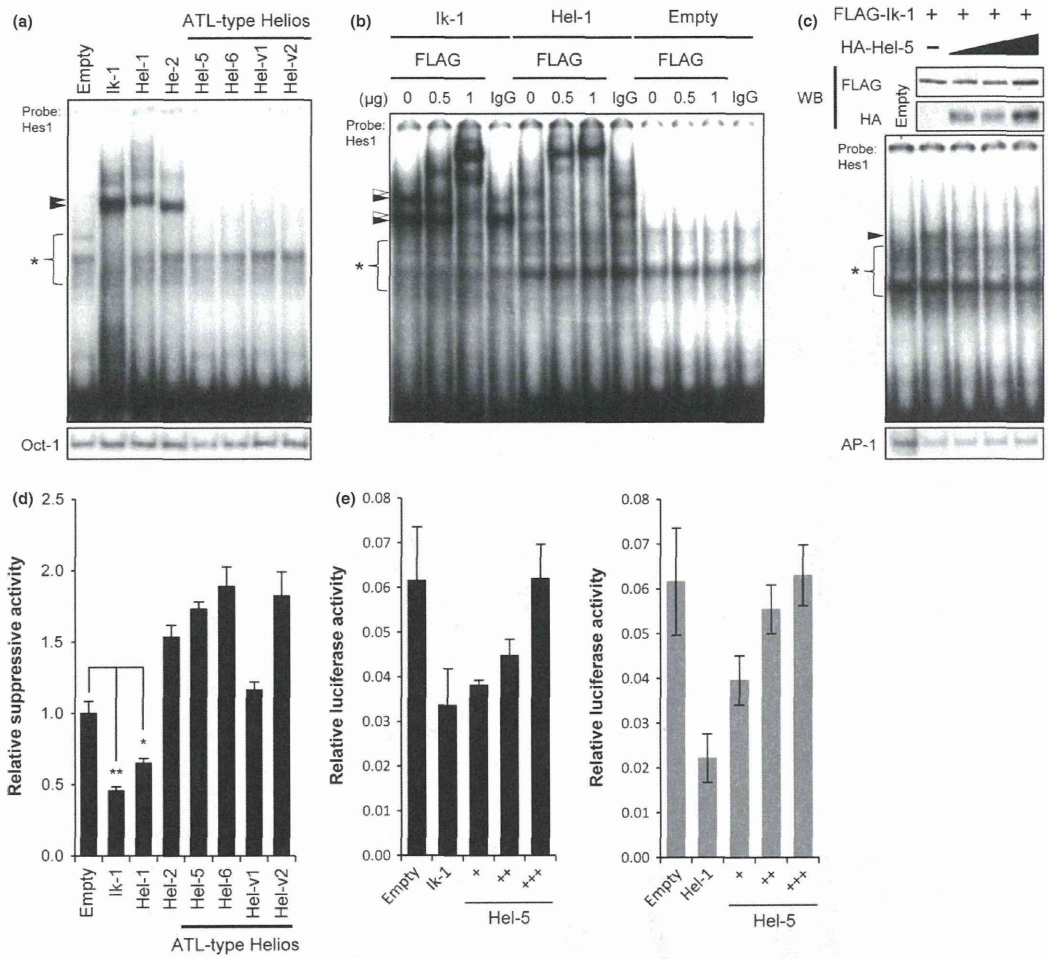

Fig. 5. Dominant-negative function of adult T-cell leukemia (ATL)-type Helios isoforms. (a) DNA-binding activities of wild-type Helios or Ikaros and ATL-type Helios proteins. Each FLAG-tagged Helios or Ikaros isoforms were ectopically expressed in 293T cells and their nuclear extracts were subjected to EMSA with a [γ-^{32}P]-labeled *Hes1* promoter probe. Oct-1 probe was used as an internal control. Arrowheads indicate Helios or Ikaros complexes. *Non-specific bands. Hel-v1, Hel-variant 1; Hel-v2, Hel-variant 2. (b) Results of supershift assays. Anti-FLAG (0, 0.5, 1 μg) or control IgG (1 μg) antibodies were added to each nuclear extract prior to electrophoresis. The black and white arrowheads indicate the supershifted bands of Ik-1 and Hel-1, respectively. (c) Antagonistic effects of Hel-5 on DNA-binding of Ik-1 tested by EMSA. The molar ratios of Ik-1 to Hel-5 plasmids are 1:1, 1:4, and 1:8. Expression levels of FLAG-Ik-1 and HA-Hel-5 were assessed by immunoblotting. The arrowheads indicate the Ik-1 specific band. AP-1 probe was used as an internal control. WB, western blot. (d) Transcriptional suppression activities of various Helios or Ikaros isoforms tested by *Hes1 promoter-luciferase reporter systems* (n = 3, mean ± SD). Basal *Hes1 promoter activity was defined as firefly/renilla ratio, and* suppression activities of Helios or Ikaros are relatively presented. Statistical significance was evaluated by unpaired Student's t-test (*P < 0.05; **P < 0.01). (e) Inhibitory function of Hel-5 against Ik-1 and Hel-1 tested by *Hes1* promoter assay (n = 3, mean ± SD). The molar ratios of Ik-1 or Hel-1 to Hel-5 plasmids are 1:1, 1:2, and 1:3. Relative luciferase activities were defined as firefly/renilla ratio.

upregulation in our ATL samples (Fig. S7). Hes1 has been reported to directly promote cell proliferation through the transcriptional repression of p27kip1.[39] Taken together, our results suggest a possibility that abnormalities in Helios expression are one of the causes of Hes1 activation, which may be one of the genetic events involved in ATL leukemogenesis.

Our results show that the Hel-5 variant may have an oncogenic role, whereas the wild-type Helios, Hel-1, shows tumor suppressor-like activity. These findings are consistent with previous findings in mice.[15] Furthermore, our description of expression profiles of stable cells followed by pathway analyses showed activation of several important pathways in lymphocytes for the regulation of proliferation, survival, and others. In particular, we discovered novel molecular cross-talk between the Ikaros family and the S1P pathway. The S1P–S1PR1 axis is known to play important

doi: 10.1111/cas.12181

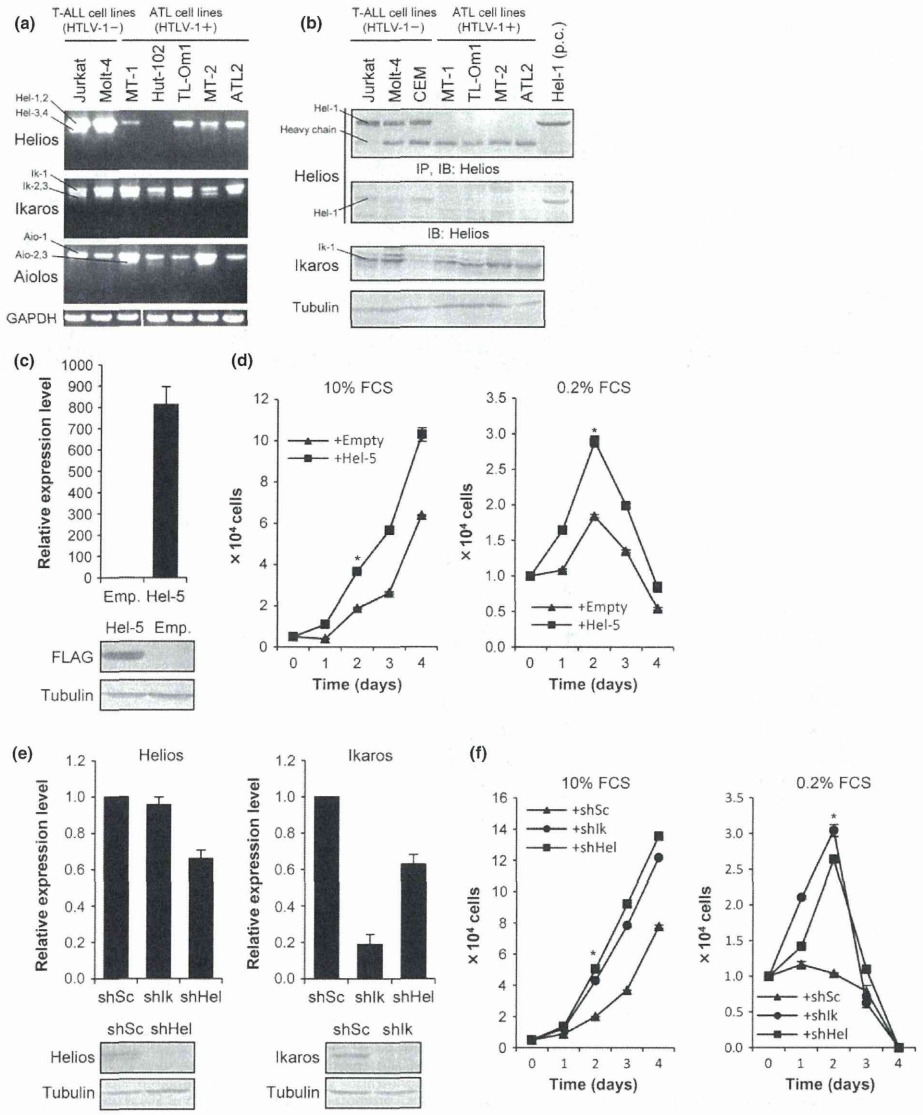

Fig. 6. Hel-5 functions in T cell growth and survival. (a) Expression patterns and levels of Ikaros family genes in various cell lines examined by RT-PCR. ATL, adult T-cell leukemia; T-ALL, acute T lymphoblastic leukemia. (b) Results of immunoblotting analyses of the immunoprecipitants (top panel) and cell lysates (lower panels). Positive control (p.c.), Hel-1 transfectant. IB, immunoblot; IP, immunoprecipitant. (c) Establishment of Jurkat cells stably expressing Hel-5. The Hel-5 level was quantified by quantitative RT-PCR (top, $n = 3$, mean ± SD) and immunoblotting (bottom). (d) Cell proliferation analysis of control cells (▲) and Hel-5-expressing Jurkat cells (■) under two FCS conditions ($n = 3$, mean ± SD). Statistical significance was observed (*P <0.01, Student's t-test). (e) Knockdown analyses of Helios or Ikaros in Jurkat cells. The Helios and Ikaros levels were evaluated by quantitative RT-PCR (top, $n = 3$, mean ± SD) and immunoblotting (bottom), respectively. (f) Cell proliferation curves of scrambled shRNA (shSc) cells (▲), shIkaros (shIk) cells (●), and shHelios (shHel) cells (■) were examined in two FBS conditions ($n = 3$, mean ± SD; *$P < 0.01$).

roles in regulation of the immune system, apoptosis, cell cycle, and migration of lymphocytes.[40–42] Recently, activation of the S1P pathway in various diseases, including leukemia, has been reported, and the therapeutic potential of S1PR1 inhibitors was suggested.[42] Studies of functional roles of S1P pathway activation in ATL cells are now underway in our laboratory.

In conclusion, our present study revealed a novel aspect of molecular abnormalities in ATL cells: a profound deregulation in Helios expression, which appears to play an important role in T-cell proliferation. Our experimental approaches also imply that, in addition to genetic and epigenetic abnormalities, ATL shows abnormal splicing, which has been observed in various human diseases including cancers.[43–45]

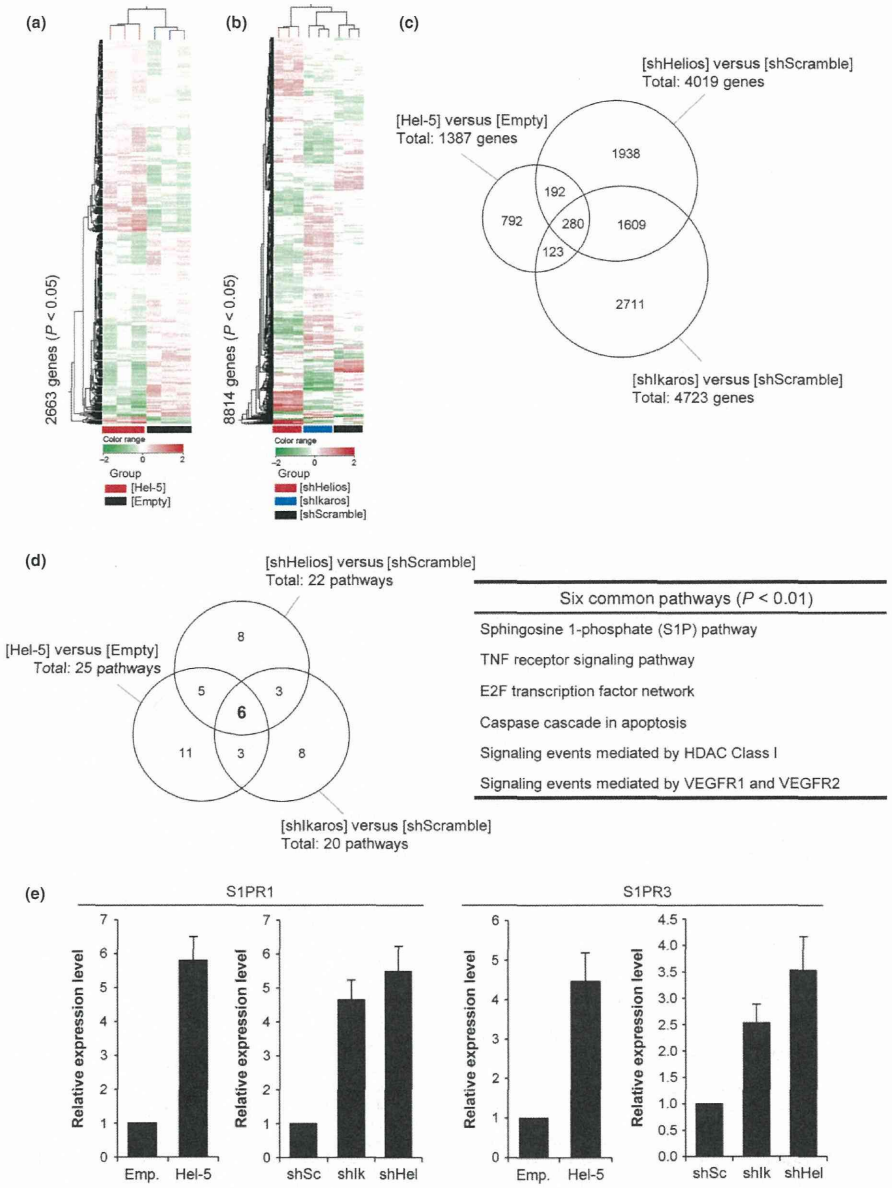

Fig. 7. Comprehensive search for Helios target genes by microarray analysis. (a,b) Gene expression analysis of Jurkat stable cells. The gene expression patterns of Jurkat cells expressing Hel-5 ($n = 3$), shIkaros ($n = 3$), and shHelios ($n = 3$) were comprehensively analyzed by microarray technique. The obtained 2D hierarchical clusters and Pearson's correlation between the cells expressing Hel-5 or not (a) and the cells introducing shHel, shIk, or shSc (b). (c) Venn diagram of differential gene expression pattern in the Jurkat sublines. The each differential expression gene set (5-fold changes, $P < 1 \times 10^{-5}$) was compared. (d) Venn diagram depicting the overlap between the outputs of pathway analysis in Jurkat sublines. The analysis was based on the NCI-Nature Pathway Interaction Database.[37] Each differential pathway set (*t*-test, $P < 0.01$) was compared and the common pathways listed. (e) Results of quantitative RT-PCR of shingosine-1-phosphate receptor 1 (S1PR1) and receptor 3 (S1PR3) in Jurkat sublines ($n = 3$, mean ± SD). HDAC, histone deacetylase; VEGFR, vascular endothelial growth factor receptor.

Acknowledgments

We thank Mr. M. Nakashima and Ms. T. Akashi for support and maintenance of the Joint Study on Prognostic Factors of ATL Development. This work is supported by JSPS KAKENHI Grant Numbers 24790436 (M.Y.), 23390250 (T.W.), 23659484 (T.W.), 23 6291 (S.A.), NEXT KAKENHI Grant Number 221S0001 (T.W.), and a Grant-in-Aid from the Ministry of Health, Labor and Welfare of Japan H24-G-004 (M.Y. and T.W.).

doi: 10.1111/cas.12181

Disclosure Statement

The authors have no conflict of interest.

References

1 Yamaguchi K, Watanabe T. Human T lymphotropic virus type-I and adult T-cell leukemia in Japan. *Int J Hematol* 2002; **76**: 240–45.
2 Iwanaga M, Watanabe T, Utsunomiya A *et al.* Human T-cell leukemia virus type I (HTLV-1) proviral load and disease progression in asymptomatic HTLV-1 carriers: a nationwide prospective study in Japan. *Blood* 2010; **116**: 1211–19.
3 Yamagishi M, Nakano K, Miyake A *et al.* Polycomb-mediated loss of miR-31 activates NIK-dependent NF-κB pathway in adult T cell leukemia and other cancers. *Cancer Cell* 2012; **21**: 121–35.
4 Yamagishi M, Watanabe T. Molecular hallmarks of adult T cell leukemia. *Front Microbiol* 2012; **3**: 334.
5 Lo K, Landau NR, Smale ST. LyF-1, a transcriptional regulator that interacts with a novel class of promoters for lymphocyte-specific genes. *Mol Cell Biol* 1991; **11**: 5229–43.
6 Georgopoulos K, Moore DD, Derfler B. Ikaros, an early lymphoid-specific-transcription factor and a putative mediator for T cell commitment. *Science* 1992; **258**: 808–12.
7 Hahm K, Ernst P, Lo K, Kim GS, Turck C, Smale ST. The lymphoid transcription factor LyF-1 is encoded by specific, alternatively spliced mRNAs derived from the Ikaros gene. *Mol Cell Biol* 1994; **14**: 7111–23.
8 Sun L, Liu A. Zinc finger-mediated protein interactions modulate Ikaros activity, a molecular control of lymphocyte development. *EMBO J* 1996; **15**: 5358–69.
9 Morgan B, Sun L, Avitahl N *et al.* Aiolos, a lymphoid restricted transcription factor that interacts with Ikaros to regulate lymphocyte differentiation. *EMBO J* 1997; **16**: 2004–13.
10 Kelley CM, Ikeda T, Koipally J *et al.* Helios, a novel dimerization partner of Ikaros expressed in the earliest hematopoietic progenitors. *Curr Biol* 1998; **8**: 508–15.
11 Cobb BS, McCarty AS, Brown KE *et al.* Helios, a T cell-restricted Ikaros family member that quantitatively associates with Ikaros at centromeric heterochromatin. *Genes Dev* 1998; **12**: 782–96.
12 Winandy S, Wu P, Georgopoulos K. A dominant mutation in the Ikaros gene leads to rapid development of leukemia and lymphoma. *Cell* 1995; **83**: 289–99.
13 Wang JH, Nichogiannopoulou A, Wu L *et al.* Selective defects in the development of the fetal and adult lymphoid system in mice with an Ikaros null mutation. *Immunity* 1996; **5**: 537–49.
14 Wang JH, Avitahl N, Cariappa A *et al.* Aiolos regulates B cell activation and maturation to effector state. *Immunity* 1998; **9**: 543–53.
15 Zhang Z, Swindle CS, Bates JT, Ko R, Cotta CV, Klug CA. Expression of a non-DNA-binding isoform of Helios induces T-cell lymphoma in mice. *Blood* 2007; **109**: 2190–7.
16 Sun L, Crotty ML, Sensel M *et al.* Expression of dominant-negative Ikaros isoforms in T-cell acute lymphoblastic leukemia. *Clin Cancer Res* 1999; **5**: 2112–20.
17 Nakase K, Ishimaru F, Avitahl N *et al.* Dominant negative isoform of the Ikaros gene in patients with adult B-cell acute lymphoblastic leukemia. *Cancer Res* 2000; **60**: 062–4065.
18 Takanashi M, Yagi T, Imamura T *et al.* Expression of the Ikaros gene family in childhood acute lymphoblastic leukaemia. *Br J Haematol* 2002; **117**: 525–30.
19 Nishii K, Katayama N, Miwa H. Non-DNA-binding Ikaros isoform gene expressed in adult B-precursor acute lymphoblastic leukemia. *Leukemia* 2002; **16**: 1285–92.
20 Tonnelle C, Imbert M-C, Sainty D, Granjeaud S, N'Guyen C, Chabannon C. Overexpression of dominant-negative Ikaros 6 protein is restricted to a subset of B common adult acute lymphoblastic leukemias that express high levels of the CD34 antigen. *Hematol J* 2003; **4**: 104–9.
21 Klein F, Feldhahn N, Herzog S *et al.* BCR-ABL1 induces aberrant splicing of IKAROS and lineage infidelity in pre-B lymphoblastic leukemia cells. *Oncogene* 2006; **25**: 1118–24.
22 Zhou F, Mei H, Jin R, Li X, Chen X. Expression of ikaros isoform 6 in chinese children with acute lymphoblastic leukemia. *J Pediatr Hematol Oncol* 2011; **33**: 429–32.
23 Mullighan CG, Miller CB, Radtke I *et al.* BCR-ABL1 lymphoblastic leukaemia is characterized by the deletion of Ikaros. *Nature* 2008; **453**: 110–14.
24 Kano G, Morimoto A, Takanashi M *et al.* Ikaros dominant negative isoform (Ik6) induces IL-3-independent survival of murine pro-B lymphocytes by activating JAK-STAT and up-regulating Bcl-xl levels. *Leuk Lymphoma* 2008; **49**: 965–73.
25 Iacobucci I, Lonetti A, Messa F *et al.* Expression of spliced oncogenic Ikaros isoforms in Philadelphia-positive acute lymphoblastic leukemia patients treated with tyrosine kinase inhibitors: implications for a new mechanism of resistance. *Blood* 2008; **112**: 3847–55.
26 Mullighan CG, Su X, Zhang J *et al.* Deletion of IKZF1 and prognosis in acute lymphoblastic leukemia. *N Engl J Med* 2009; **360**: 470–80.
27 Kuiper RP, Waanders E, van der Velden VHJ *et al.* IKZF1 deletions predict relapse in uniformly treated pediatric precursor B-ALL. *Leukemia* 2010; **24**: 1258–64.
28 Nakase K, Ishimaru F, Fujii K *et al.* Overexpression of novel short isoforms of Helios in a patient with T-cell acute lymphoblastic leukemia. *Exp Hematol* 2002; **30**: 313–17.
29 Fujii K, Ishimaru F, Tabayashi T *et al.* Over-expression of short isoforms of Helios in patients with adult T-cell leukaemia/lymphoma. *Br J Haematol* 2003; **120**: 986–9.
30 Fujiwara SI, Yamashita Y, Nakamura N *et al.* High-resolution analysis of chromosome copy number alterations in angioimmunoblastic T-cell lymphoma and peripheral T-cell lymphoma, unspecified, with single nucleotide polymorphism-typing microarrays. *Leukemia* 2008; **22**: 1891–8.
31 Fujimoto R, Ozawa T, Itoyama T, Sadamori N, Kurosawa N, Isobe M. HELIOS-BCL11B fusion gene involvement in a t(2;14)(q34;q32) in an adult T-cell leukemia patient. *Cancer Genet* 2012; **205**: 356–64.
32 Shimoyama M. Diagnostic criteria and classification of clinical subtypes of adult T-cell leukaemia-lymphoma. A report from the Lymphoma Study Group (1984–87). *Br J Haematol* 1991; **79**: 428–37.
33 Tabayashi T, Ishimaru F, Takata M *et al.* Characterization of the short isoform of Helios overexpressed in patients with T-cell malignancies. *Cancer Sci* 2007; **98**: 182–8.
34 Kathrein KL, Chari S, Winandy S. Ikaros directly represses the notch target gene Hes1 in a leukemia T cell line: implications for CD4 regulation. *J Biol Chem* 2008; **283**: 10476–84.
35 Kleinmann E, Geimer Le Lay AS, Sellars M, Kastner P, Chan S. Ikaros represses the transcriptional response to Notch signaling in T-cell development. *Mol Cell Biol* 2008; **28**: 7465–75.
36 Molnár A, Georgopoulos K. The Ikaros gene encodes a family of functionally diverse zinc finger DNA-binding proteins. *Mol Cell Biol* 1994; **14**: 8292–303.
37 Schaefer CF, Anthony K, Krupa S *et al.* PID: the pathway interaction database. *Nucleic Acids Res* 2009; **37**: D674–9.
38 Pancewicz J, Taylor JM, Datta A. Notch signaling contributes to proliferation and tumor formation of human T-cell leukemia virus type 1-associated adult T-cell leukemia. *Proc Natl Acad Sci USA* 2010; **107**: 16619–24.
39 Murata K, Hattori M, Hirai N *et al.* Hes1 directly controls cell proliferation through the transcriptional repression of p27Kip1. *Mol Cell Biol* 2005; **25**: 4262–71.
40 Maeda Y, Seki N, Sato N, Sugahara K, Chiba K. Sphingosine 1-phosphate receptor type 1 regulates egress of mature T cells from mouse bone marrow. *Int Immunol* 2010; **22**: 515–25.
41 Spiegel S, Milstien S. The outs and the ins of sphingosine-1-phosphate in immunity. *Nat Rev Immunol* 2011; **11**: 403–15.
42 Maceyka M, Harikumar KB, Milstien S, Spiegel S. Sphingosine-1-phosphate signaling and its role in disease. *Trends Cell Biol* 2012; **22**: 50–60.
43 Ghigna C, Valacca C, Biamonti G. Alternative splicing and tumor progression. *Curr Genomics* 2008; **9**: 556–70.
44 David CJ, Manley JL. Alternative pre-mRNA splicing regulation in cancer: pathways and programs unhinged. *Genes Dev* 2010; **24**: 2343–64.
45 Blair CA, Zi X. Potential molecular targeting of splice variants for cancer treatment. *Indian J Exp Biol* 2011; **49**: 836–9.

Supporting Information

Additional Supporting Information may be found in the online version of this article:

Fig. S1. Deregulated expression of Ikaros family genes in primary adult T-cell leukemia cells.

Effects of riboflavin and ultraviolet light treatment on platelet thrombus formation on collagen via integrin αIIbβ3 activation

Chikahiro Terada, Junpei Mori, Hitoshi Okazaki, Masahiro Satake, and Kenji Tadokoro

BACKGROUND: The adoption of pathogen reduction technology (PRT) is considered for the implementation of safer platelet (PLT) transfusion. However, the effects of PRT treatment on PLT thrombus formation under blood flow have not yet been fully clarified.

STUDY DESIGN AND METHODS: Leukoreduced PLT concentrates (PCs) obtained by plateletpheresis were treated with riboflavin and ultraviolet light (Mirasol PRT). PC samples were passed through a column filled with collagen-coated beads at a fixed shear rate after 1, 3, and 5 days of storage. The thrombus formation ability was evaluated by measuring collagen column retention rate. The change in the activation state of integrin αIIbβ3 on PLTs during storage was examined by flow cytometry.

RESULTS: The retention rate of the PRT-treated PLTs was significantly higher than that of the control PLTs on the day of treatment and decreased with storage but remained higher than those of the control during storage. This modification did not correlate with the total αIIbβ3 or fibrinogen binding on the PLTs but correlated significantly with PAC-1 binding. Mn^{2+}-induced αIIbβ3 activation also fully restored the retention rate in the Day 5 PRT-treated PLTs along with the increase in PAC-1 binding.

CONCLUSION: Riboflavin-based PRT treatment of PCs leads to the enhancement of thrombus formation on collagen, which is related to the activation status of αIIbβ3, which does not bind to fibrinogen but binds to PAC-1. The impact of this finding on the hemostatic or even thrombogenic potential in vivo must await clinical evaluation.

The safety of blood transfusion has been improved markedly owing to advances in blood donor selection and blood testing. Concerns still exist, however, because of a relatively high incidence of bacterial contamination of platelet (PLT) products and the possible risk of transfusion-transmitted infection by emerging pathogens.[1] Therefore, the adoption of pathogen reduction technologies (PRTs) that broadly and nonspecifically inactivate pathogens is being considered in many countries for the implementation of safer PLT transfusions. Current PRTs are based on inactivation methods using ultraviolet (UV) light irradiation with or without a photosensitizing agent against pathogen nucleic acids.[2] The Mirasol PRT system (Terumo BCT, Tokyo, Japan) uses UV light (265-370 nm) and a photosensitizing agent, riboflavin.[3] It is currently approved in some European countries for the treatment of PLT concentrates (PCs) in plasma or additive solution.[4]

Although PRT treatment enhances the safety of PCs, there are concerns about the decrease in product quality.[5] In vitro quality measurements of PCs during the storage period revealed a contribution of the PRT treatment to the PLT storage lesion when compared with the untreated controls. A decrease in pH, increase in P-selectin expression level, and decline in swirling were observed in PRT-treated PLTs.[6] In addition, the enhancement of glucose

ABBREVIATIONS: AP = apheresis; PC(s) = platelet concentrate(s); PRP = platelet-rich plasma; PRT(s) = pathogen reduction technology(-ies); TRAP = thrombin receptor–activating peptide.

From the Department of Research and Development, Central Blood Institute, Japanese Red Cross Society, Tokyo, Japan.

Address reprint requests to: Chikahiro Terada, Department of Research and Development, Central Blood Institute, Japanese Red Cross Society, 2-1-67 Tatsumi, Koto-ku, Tokyo 135-8521, Japan; e-mail: c-terada@jrc.or.jp.

Received for publication May 1, 2013; revision received November 29, 2013, and accepted December 2, 2013.

doi: 10.1111/trf.12566

TRANSFUSION **;**:**-**.